ELSEVIER

Surface Science 348 (1996) 227–242

surface science

Conventional and manipulated growth of Cu/Cu(111)

Wulf Wulfhekel [a,*], Nuphar N. Lipkin [a], Jörg Kliewer [a], Georg Rosenfeld [a], Louis C. Jorritsma [b], Bene Poelsema [b], George Comsa [a]

[a] *Institut für Grenzflächenforschung and Vakuumphysik, KFA-Forschungszentrum Jülich GmbH, D–52425 Jülich, Germany*

[b] *Faculty of Applied Physics and Centre for Materials Research (CMO), University of Twente, P.O. Box 217, 7500 AE Enschede, The Netherlands*

Received 19 July 1995; accepted for publication 25 September 1995

Abstract

Molecular beam epitaxy of Cu on Cu(111) was studied using thermal energy He scattering, in the temperature range between 100 and 450 K. Three-dimensional growth was observed in the whole temperature range. To determine the onset of various diffusion processes, submonolayer films formed by deposition at low temperature were annealed. Annealing proceeds in two steps. The first step is interpreted as a change in island shape, the second as Ostwald-ripening. A comparison with homoepitaxy on Pt(111) and Ag(111) is made. Growth manipulation was carried out by artificially increasing the island number density via intervention in the nucleation stage of each layer. The procedures applied were temperature reduction during nucleation as well as pulsed ion bombardment. These techniques enabled the convenient growth of good quality films consisting of a large number of monolayers. Finally, the use of oxygen as a surfactant modifying the growth mode was investigated. Under some growth conditions, pre-exposure of the surface to oxygen was found to induce weak He-intensity oscillations during deposition. The quality of the films grown in this way was, however, low.

Keywords: Atom–solid scattering and diffraction – elastic; Copper; Growth; Ion bombardment; Metallic surfaces; Molecular beam epitaxy; Oxygen; Surface diffusion

1. Introduction

Homoepitaxial systems can be used as model systems, where simple kinetic processes influencing epitaxial growth can be studied without complicating effects such as lattice mismatch, differences in surface energy, etc. A detailed understanding of the origin of the various phenomena occurring in homoepitaxy, as well as the development of general concepts and the identification of general trends are important for deriving from these simpler systems conclusions applicable to the more complex, and more useful, heteroepitaxial systems.

Such general trends seem to apply for homoepitaxy on fcc (100) metal surfaces, for which layer-by-layer growth is generally found (Pd [1], Ni [2], Cu [3,4], Ag [4–7]). For homoepitaxy on fcc(111) metal surfaces the situation is more complex. The two model systems studied extensively – Pt/Pt(111) and Ag/Ag(111) – display a richness of behaviour, depending on the growth conditions (substrate temperature, deposition rate) and on the metal.

For homoepitaxy on Pt(111), three growth regimes were observed at temperatures below

* Corresponding author. Fax: +49 2461 613907; E-mail: w.wulfhekel@kfa-juelich.de.

SSDI 0039-6028(95)00988-4

step-flow [8–12]: at intermediate temperatures (340–450 K), several layers grow simultaneously and the system grows three-dimensionally rough (3D growth). This mode of growth was explained by the existence of a barrier (step-edge barrier [13,14]), hindering interlayer mass transport. At lower temperatures, a non-ideal layer-by-layer growth mode (reentrant 2D growth) is encountered, which was explained by the partial enabling of interlayer mass transport due to the fractal-like shape of the islands growing at these temperatures. At high temperatures, growth proceeds in an almost ideal layer-by-layer manner for a very large number of monolayers. This latter growth mode was explained initially by an increased probability for adatoms to thermally surmount the step-edge barrier. Recently, an alternative mechanism was proposed, tracing back this growth mode to a reconstruction network forming on the Pt(111) surface during deposition [15,16]. Scanning tunnelling microscopy (STM) investigations [16] showed that those parts of the surface which are not reconstructed grow three-dimensionally.

Ag growing on Ag(111) shows a very different behaviour [6,12,17–19]. For this system, the growth is three-dimensional at all temperatures below step-flow, indicative of a high step-edge barrier.

For the third fcc(111) system studied so far – Cu/Cu(111), conflicting results were reported. A behaviour similar to that of Ag/Ag(111) has been observed by Dastoor and co-workers [20,21], whereas a behaviour similar to that of Pt/Pt(111) was found by Henzler and co-workers [12,22,23].

The first part of this paper (Section 3.1) is devoted to the investigation of the conventional homoepitaxial growth on Cu(111), in order to resolve this discrepancy and gain a more general overview on the growth in fcc(111) systems.

The second part of the paper deals with growth manipulation in the Cu/Cu(111) system, leading to much smoother films than those grown using conventional procedures. Manipulation is based on the "concept of two mobilities" [24,25] which has been developed in our group and applied previously to the growth of Ag on Ag(111) [17]. In these manipulation techniques, an artificially high density of islands is produced during the nucleation stage of each monolayer, such that the typical distance between two such islands is smaller than the "free-diffusion length" of adatoms at the growth temperature and deposition rate used (i.e. smaller than the average length that an adatom can travel on the surface before it collides with other adatom(s) to form a stable nucleus). Adatoms landing from the gas phase on these islands will therefore be able to reach the edge of the islands and attempt to surmount the step edge barrier much more frequently than adatoms landing on the larger islands formed during natural growth. The probability of surmounting the barrier and reaching the lower terrace before forming a stable nucleus on top of a pre-existing island is proportional to the number of attempts, and is thus greater the smaller the typical island size is.

Artificially enhanced island density during nucleation was produced in several ways. Section 3.2.1 presents the results of experiments where an enhanced island density was produced by lowering the substrate temperature during the nucleation stage of monolayer growth, Section 3.2.2 presents the results of experiments in which this aim was achieved by ion bombardment at that stage. An assessment of the quality of the grown layers and of the degree to which the island density must be increased in order to achieve high-quality layers is given.

In addition, Section 3.3 presents results of experiments where growth was influenced by pre-exposing the copper surface to molecular oxygen. This procedure results in an (imperfect) layer-by-layer growth of several monolayers. A mechanism for the influence of oxygen is proposed.

2. Experimental set-up

The experiments described in this paper were carried out in an ultra-high-vacuum (UHV) chamber with base pressure below 5×10^{-11} mbar. The system has been described in detail elsewhere [26,27]. A 67 meV supersonic He beam was used for the He scattering measurements. The transfer-width at the experimental conditions was ~ 420 Å [28]. The scattering apparatus was also equipped with an Auger electron spectrometer (AES).

Sample temperature was measured using a Ni–CrNi thermocouple inserted into a cavity in the crystal.

The sample was prepared by repeated cycles of sputtering with 1.2 keV Ne^+-ions and annealing to 1000 K. This procedure was repeated until no contamination could be detected by means of AES and the He reflectivity from the surface was high. The estimated mean terrace width on the surface was over 1000 Å. After each deposition experiment, the initial conditions were recovered by sputtering and annealing to 850 K.

Copper was evaporated onto the sample from a high purity Cu disk which was thoroughly desulphurised and outgassed. A home made electron bombardment evaporator was used. During deposition the pressure stayed below 1×10^{-10} mbar. The deposition rate was determined from the frequency of He intensity oscillations under conditions where layer-by-layer growth was obtained.

The specularly reflected He beam under in- or anti-phase conditions was recorded in situ during deposition. Under in-phase scattering condition, interference from adjacent layers is constructive. The sample thus looks like a perfect mirror except for impurities and a strip about 10 Å wide around step edges, which scatter diffusively. Therefore, variations in the He intensity during deposition reflect the variation in the step edge length per unit area on the surface during growth [26]. Under anti-phase scattering condition interference from adjacent layers is destructive. The anti-phase intensity is therefore indicative of the height distribution of the growing film [26]. It is only in specific cases, however, that the height distribution can be uniquely determined from the anti-phase intensity. Similarly to the in-phase intensity, also the anti-phase intensity is reduced by diffuse scattering due to the presence of defects on the surface.

At temperatures where the adatoms are mobile, ideal three-dimensional growth is due to the complete lack of interlayer mass transport. For this type of growth, both in- and anti-phase He intensities decay monotonically. The normalized anti-phase intensity follows an exponential decay law $I^{anti}/I_0^{anti}=e^{-4\theta}$, where θ is the coverage in monolayers (ML) [26]. During layer-by-layer growth mass transport between layers is efficient, resulting in oscillations of the He intensity under both diffraction conditions. The minimum intensity corresponds to deposition of about 0.5 ML, when the surface is roughest. The maximum intensity corresponds roughly to completion of a layer.

Mean terrace widths were estimated by comparing the reflected He intensities under in- and anti-phase conditions [29]. Mean island separations were estimated from the broadening of He peak profiles under anti-phase conditions [30,31]. Peak profiles were recorded by changing the angle of the sample with respect to the detector after quenching the sample temperature to 200 K following deposition.

Oxygen experiments were carried out using molecular oxygen 4.8 which was let in through a leak valve. Partial pressures up to a maximum of 2×10^{-7} mbar were used.

3. Results and discussion

3.1. Conventional growth of Cu/Cu(111) and annealing

The normalized specularly reflected He intensities under anti-phase diffraction conditions ($n=2.5$) were recorded for different substrate temperatures as a function of deposition time. Deposition was carried out at a rate of $R=0.006$ ML/s for all temperatures. The results are shown in Fig. 1.

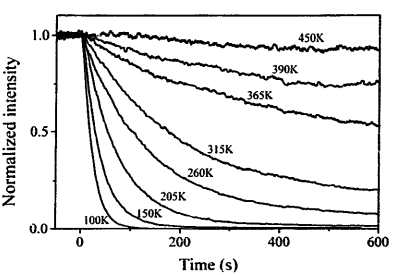

Fig. 1. Evolution of the normalized specular He intensity under anti-phase conditions ($n=2.5$) during deposition of Cu onto Cu(111) at different substrate temperatures, as indicated. Deposition was carried out at a rate of $R=0.006$ ML/s.

For the highest temperature chosen ($T=450$ K), the intensity remains about constant during deposition. This indicates growth by step flow. At this high temperature the mobility of the adatoms is high enough, such that all adatoms landing on the pre-existing terraces diffuse to the ascending step edges, where they are captured before they nucleate. Hence, no nucleation of islands is taking place on the terraces and the film grows via propagation of the pre-existing steps [32]. The onset temperature of ideal step flow growth is, however, not an intrinsic property of the material. It is also determined by the average terrace width of the surface and hence the crystal surface quality.

At lower temperatures the intensity falls monotonically during deposition, typical for 3D growth. Note that for the curve obtained at 100 K, the rate of decay is steeper than that expected for ideal 3D growth ($I^{anti}/I_0^{anti}=e^{-\Theta}$). This is due to diffuse scattering from small structures as will be discussed at the end of this section. Between the two extremes, 3D growth at low temperatures and step flow at high temperature, a gradual transition is found.

None of the curves displays oscillations of the intensity during deposition. This indicates that growth does *not* proceed in a layer-by-layer fashion at any temperature. The fact that the intensity decays monotonically even at elevated temperatures (>300 K), i.e. three-dimensional structures are formed, shows that interlayer mass transport is considerably hampered by the existence of a barrier for downward diffusion over a step edge.

The high temperature oscillations observed for Cu/Cu(111) with spot profile analysis low energy electron diffraction (SPA-LEED) ($T=370$ K, $R=$ 0.8 ML/min and 3 ML/min) [12,22,23] could not be reproduced in our He scattering experiments. It is unlikely that the discrepancy is due to differences in the average terrace width, as both surfaces were of similar quality. It is also not likely that the different transfer widths of the two diffraction techniques (about 400 Å for TEAS and 1000–2000 Å for SPA–LEED) is responsible for the contradicting results. The very pronounced oscillations observed in the SPA–LEED experiments should have been observable also with He scattering. In addition, preliminary SPA–LEED experiments with our crystal did not show intensity oscillations under the conditions used in Refs. [12,22,23]. The reported oscillations were found to be accompanied by a widening in SPA–LEED anti-phase peak profiles taken from the surface during growth with respect to peak profiles recorded during growth at lower temperatures [33]. The structures growing during the high-temperature oscillations are thus smaller than structures growing at lower temperatures. Such a behaviour is not expected on the basis of nucleation theory [34,35] and can therefore not be explained by homogeneous nucleation. Further experiments are needed in order to fully resolve the discrepancy.

In the light of our observations, it seems that a high step-edge barrier is in general a common feature of the (111) face of fcc noble metals, as both Cu(111) and Ag(111) [6,12,17–19] grow three-dimensionally for all temperatures below step flow, and Pt(111) grows in the same mode for a wide temperature range [8–11]. The 2D growth of Pt(111) at higher temperatures seems to be an exception which can be traced back to the reconstruction of the Pt surface. The reconstruction network reduces the mobility of adatoms on the surface and leads to an enhanced density of nuclei during the early stages of each monolayer growth [15,16]. In the absence of this reconstruction, also Pt grows 3D at high temperatures [16].

Like in the homoepitaxial system Ag/Ag(111), no reentrant oscillations could be found for Cu/Cu(111) with He scattering. In LEED measurements, however, low-scale reentrant oscillations were observed at low temperatures [12]. The oscillations were of very low amplitude (e.g. for a surface temperature of 172 K and a deposition rate of $R=0.03$ ML/s, the amplitude of the first and highest oscillation is 0.005 of the initial LEED intensity [33]). At these low temperatures we find a strong decay of the in-phase He intensity during growth, indicating substantial diffuse scattering from small structures on the surface. This strong diffuse scattering causes an additional damping of the anti-phase He intensity, which could lead to a lower sensitivity of TEAS to such small oscillations. A reduced sensitivity of TEAS to low temperature oscillations was encountered for several other systems. RHEED oscillations during low-temperature

growth of Ag/Ag(100) [6] and Cu/Cu(100) [3] are much more pronounced than the equivalent TEAS oscillations for these systems [7,36], whereas the high temperature oscillations are of equal quality. The discrepancy between LEED and TEAS measurements at low temperatures are most likely due to this effect.

Nevertheless, even if low-scale reentrant oscillations are present, it is clear that neither Cu/Cu(111) nor Ag/Ag(111) displays such pronounced reentrant oscillations as Pt/Pt(111) does, where the amplitude of the first oscillation is 0.5 of the initial He intensity [8]. The existence of the reentrant layer-by-layer growth mode in Pt/Pt(111) was explained by a transition in the island shapes from compact at higher temperatures to dendritic at low temperatures. However, such a transition in island shapes is present also in Ag/Ag(111) [17] and in Cu/Cu(111), as will be shown at the end of this section. This indicates that a transition in island shape alone is not a sufficient condition for the occurrence of reentrant layer-by-layer growth. The behaviour of Pt/Pt(111) also at low temperatures seems to be the exception rather than the rule. Simulations point out that the reentrant layer-by-layer growth on Pt(111) may be promoted by an exceptionally low barrier for an exchange process at kink sites, leading to efficient interlayer mass transport at irregularly-shaped islands [37,38]. A series of corrected effective medium (CEM) calculations for the three systems [39,40] indicated that for Pt adatoms diffusing on Pt(111) the potential energy barrier for interlayer diffusion by an exchange mechanism at the edge of small (10–60 atoms) compact islands is actually lower than the barrier for terrace diffusion, whereas for Ag/Ag(111) and Cu/Cu(111) the situation is reversed. Both calculations emphasize the importance of a diffusion behaviour unique to Pt/Pt(111) in the occurrence of the pronounced reentrant layer-by-layer growth mode for Pt/Pt(111). The exceptionally low barriers for diffusion by exchange are in accord with the tendency of the Pt(111) surface to reconstruct by adatom incorporation into the topmost surface layer.

To complete our study on the unmanipulated growth of Cu/Cu(111) we investigate the annealing of structures obtained by growth at low temperatures. First, 0.1 ML were deposited at 100 K with a rate of $R=0.006$ ML/s. At this low coverage the islands would be predominantly two-dimensional, even in the presence of a high barrier for interlayer mass transport. Following deposition the substrate is heated at a constant rate of 10 K/min while monitoring the in- or anti-phase He intensity. The resulting intensities, normalized to unity before deposition and corrected for Debye–Waller effects, are shown as a function of temperature in Fig. 2a.

At about 200 K, both in- and anti-phase intensities start to increase until at about 250 K a plateau is reached, which indicates that a first annealing step has taken place. Around 350 K the onset of a second annealing step is observed: both intensities rise again and at ~400 K the initial intensity values corresponding to a freshly prepared surface are reached. A similar behaviour has already been observed for Ag/Ag(111) (see Fig. 2b), and the two steps have been interpreted as a transition in the island shape from fractal to compact and Ostwald-ripening, respectively [17]. Here we will look in more detail to these annealing steps and try to substantiate this interpretation.

The two annealing steps are essentially different processes. This is evident from the fact that during the first (lower temperature) step the increase of the in-phase intensity is much larger than that of the anti-phase intensity, while during the second step the situation is reversed.

The intensity behaviour during the first annealing step is in accord with a transition in island shape. The strong rise of the in-phase intensity is expected if fractal islands which give rise to strong diffuse scattering collapse to a compact shape with straight edges. The anti-phase intensity, on the other hand, is more sensitive to the layer distribution on the surface. It does not increase much during the first annealing step, but does so during the second. The second annealing step can thus be identified as Ostwald-ripening, where larger islands grow at the expense of small ones, which decompose. This ripening process is completed when few very large islands have formed or, on a real surface, when all material on the terraces has been captured by the pre-existing step edges. The surface thus becomes effectively a one-layer system within the transfer width.

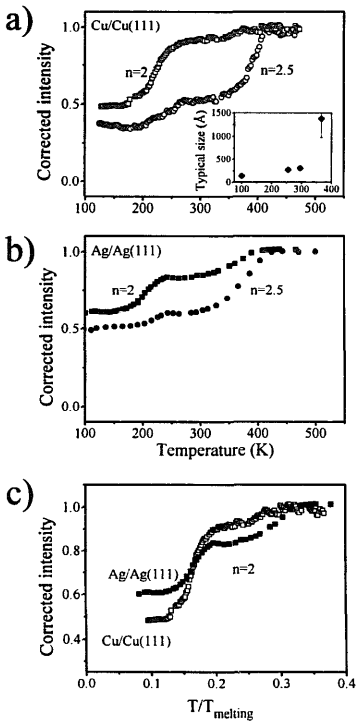

Fig. 2. (a) Debye–Waller corrected in-phase $n=2$ (squares) and anti-phase $n=2.5$ (circles) intensities during annealing of 0.1 ML Cu, deposited onto Cu(111) at 100 K, as a function of substrate temperature. The typical sizes of the structures on the surface during annealing are shown in the inset. Sizes were evaluated from the broadening of anti-phase peak profiles. The given error bar represents the error resulting from fitting the peak profiles. For the low temperatures the error is smaller than the symbol. (b) Debye–Waller corrected in-phase $n=2$ (squares) and anti-phase $n=2.5$ (circles) intensities during annealing of 0.1 ML Ag, deposited onto Ag(111) at 100 K, as a function of substrate temperature. (c) Debye–Waller corrected in-phase $n=2$ intensities during annealing of 0.1 ML Ag, deposited onto Ag(111) (filled symbols) and 0.1 ML Cu deposited onto Cu(111) (hollow symbols) at 100 K, as a function of $T/T_{melting}$.

To verify the origin of the first annealing step, anti-phase He peak profiles were recorded during annealing. The profiles consist of a central spike and a broadening [30,31]. From the shape and width of the broadening a characteristic length scale of the growth structures can be obtained. For compact two-dimensional islands the characteristic length is the mean island separation. For fractal shaped islands, however, intra-island correlations strongly influence the broadening so that the observed length scale is smaller than the island separation. The characteristic length scales during the various stages of annealing are shown in the inset of Fig. 2a. A clear rise of the length scale can be seen between 300 and 400 K corresponding to Ostwald-ripening. Between 100 and 300 K however, the length scale increases only slightly from ~ 150 to ~ 300 Å. Assuming that during the first annealing step the island shape remains the same, this slight change in the characteristic length could by no means explain the steep rise in the in-phase intensity (see Fig. 2a). The normalized in-phase intensity I^{in}/I_0^{in} is given by $I^{in}/I_0^{in}=(1-DS)^2$, where S is the step length per unit area and D the cross section for diffuse scattering of a step edge [26]. The change of length scale alone, not accompanied by changes of the island shape would result in a rise of only ~ 0.1 in the normalized in-phase intensity. Hence the shape of the islands must have changed during the first annealing step. Similar arguments hold for Ag/Ag(111).

The transformation of shape is also indicated in experiments by Meyer and co-workers [41], although the data were not interpreted in this way originally. These authors studied growth of multilayer films of Cu on Cu(111) using SPA–LEED. For growth below 185 K they observed a rotational symmetry of the anti-phase SPA–LEED peak profiles, which is typical of irregularly shaped islands. Growth at higher temperatures, however, leads to peaks of six-fold symmetry indicating compact islands with straight edges. Although the situation during growth and annealing is not the same, the transition from fractal to compact islands is determined in both cases by the onset of edge diffusion. Pronounced adatom evaporation from islands, necessary for Ostwald-ripening, sets in at higher temperatures.

In summary, a two step annealing process was

observed. During the first step, edge diffusion becomes active and the island shape changes from fractal to compact. During the second step, adatoms can evaporate from islands leading to Ostwald-ripening.

Comparing the in-phase annealing data of Cu/Cu(111) to those obtained for Ag/Ag(111) (see Fig. 2c), one finds that the temperatures where the first and second annealing steps take place scale approximately with the melting temperature ($T^{Ag}_{melting}=1234$ K, $T^{Cu}_{melting}=1356$ K). This is expected on the basis of "rule of thumb" argumentation for bond-breaking processes on the surface.

Such a "rule of thumb" scaling of activation energies is more or less confirmed by effective medium theory (EMT) calculations for Ag(111) and Cu(111) [42]. There is, however, one exception: the energy barrier for adatom diffusion on a flat terrace is found to be lower on Cu(111) than on Ag(111). Interestingly, we arrive at the same conclusion from our data, if we assume that during the first annealing step the island density remains indeed unchanged. As it is unlikely that the cross-section for diffuse scattering is much different for the two systems, the higher in-phase intensity after the first annealing step in Fig. 2c for Cu(111) indicates a lower island density, and hence, a higher adatom mobility. This is not contradicted by the fact that the intensity directly after deposition, i.e., before the first annealing step, is lower for the Cu system: edge diffusion on Cu(111) does have a higher energy barrier than on Ag(111), such that the islands are expected to be more ramified leading to more diffuse scattering.

Terrace diffusion on Cu(111) seems to be exceptionally effective. For example, an estimate of the size of the structures resulting from growth at 300 K obtained by comparing in- and anti-phase intensities at 0.5 ML coverage, results in a mean terrace width of $\sim$600 Å. The three-dimensional islands that grow at room temperature must therefore have a typical separation of over 1200 Å, corresponding to only one island per average terrace width of the substrate.

An estimate for the diffusion energy can be obtained from an analysis of the island density as a function of temperature, based on nucleation theory [34,35]. In the case where the dimer is the smallest stable nucleus, the island density n is given by $n \propto \exp(-E_d/3kT)$ where E_d is the diffusion energy, k the Boltzmann factor and T the temperature. Under the same assumption as above, i.e., an unchanged island density after the first annealing step, the island density can be obtained by evaluating peak profiles taken from surfaces onto which submonolayer amounts of Cu are deposited, followed by annealing beyond the first annealing step to make the islands compact. Fig. 3. shows an Arrhenius plot of the island number density obtained in this manner as a function of temperature in the range 55 to 140 K. 0.1 ML Cu were deposited at the temperatures indicated, followed by annealing to 273 K and additional deposition of 0.2 ML at that temperature. The additional material deposited at the higher temperature diffuses to pre-existing islands and is therefore not likely to change the island-density. A fit to the four lowest temperatures shown in Fig. 3, where the dimer is expected to be stable, gives a very low diffusion energy of $0.03^{+0.01}_{-0.005}$ eV. This low value is in accord with calculations for terrace diffusion barriers for Cu/Cu(111) (0.04 eV [40]; 0.053 eV [42]). Nevertheless, the measured value is surprisingly low. It is possible that, in contrast to our assumption, some Ostwald-ripening does take place during the annealing to 273 K, particularly for very ramified islands. The diffusion barrier might therefore be somewhat larger than this value.

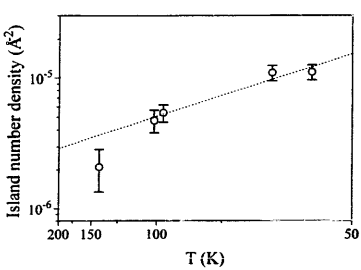

Fig. 3. Arhenius plot of the mean island density as a function of temperature for Cu islands grown on Cu(111). Deposition was carried out at a rate of $R=0.006$ ML/s.

3.2. Manipulation of growth in the Cu/Cu(111) system

A few monolayers of Cu deposited onto Cu(111) at room temperature form a film composed of large-scale (~ 600 Å) structures several monolayers high. The multi-layer growth is due to the high probability that Cu atoms landing on top of islands will nucleate to form a higher layer before they can surmount the energy barrier at the island edge and fill the lower one.

The growth manipulation procedures described in the following are aimed at reducing the probability for nucleation on top of existing islands. These procedures intervene with the nucleation stage of each monolayer, such that the mean distance between the nucleating islands is smaller than the distance which would have evolved naturally under the conditions prevailing during the further stages of monolayer growth. Once nucleation is achieved, intervention is stopped, and growth proceeds further undisturbed. The mean distance which an adatom can traverse during the later stages of monolayer growth before it collides with other adatom(s) to form a stable nucleus is thus larger than the mean distance between the islands formed during the nucleation stage. Adatoms landing on top of these islands prior to coalescence can therefore reach the edge of the island much more frequently, and the probability that they surmount the step edge barrier and fill the lower layer (2D growth) before nucleating to form a higher one (3D growth) is greatly increased.

3.2.1. Growth manipulation via temperature alternation

In this procedure, an increased island density is achieved by decreasing the substrate temperature during the nucleation stage. According to nucleation theory [34,35], the mean island separation shrinks (at least) exponentially with decreasing temperature. A reduction of the temperature during the nucleation stage therefore reduces the mean island separation quite effectively.

After nucleation, the temperature of the substrate was increased, and subsequent growth was carried out at 300 K. As this temperature lies below the onset of major Ostwald-ripening, the island density created at the nucleation stage is not much affected by coarsening during heating.

Fig. 4 shows the evolution of the anti-phase He intensities during a series of growth experiments of Cu on Cu(111) at 300 K, on surfaces which were prepared by pre-deposition of 0.05 ML Cu at lower temperatures between 200 and 100 K as indicated. The plot on the leftmost panel of Fig. 4 is the result obtained during conventional growth, i.e., where the temperature during nucleation and subsequent growth was the same. The starting intensity of all plots was normalized to the intensity reflected from a freshly prepared surface at 300 K.

From the series of results shown in Fig. 4 it is clear that the features indicative of layer-by-layer growth, namely the decrease of the specularly scattered intensity upon deposition of 0.5 ML and its rise towards the completion of a monolayer develop gradually as the pre-deposition temperature is lowered.

The 1 ML film grown on a surface which was prepared by pre-deposition at the lowest temperature, 100 K, is quite flat. The anti-phase scattered intensity after deposition of a full monolayer corresponds to the first layer being more than 95% filled, assuming a three-layer system (substrate, first layer and second layer) and an ideal instrument [43]. Thus the growth is almost ideal layer-by-layer. This indicates that the length scale imposed during the nucleation stage at this low temperature is small enough to almost completely suppress nucleation on top of the pre-existing islands during growth at 300 K and ensure effective interlayer mass transport.

The quality of the layer deposited at 300 K deteriorates with increasing predeposition temperature, as is evident from the decrease in the height of the intensity maximum upon 1 ML deposition. This deterioration reflects the fact that as the length scale imposed during nucleation increases, the islands are no longer small enough to completely suppress nucleation on top of them prior to coalescence.

The mean island separation for a film grown at 300 K after pre-deposition at 100 K inferred from an analysis of the peak profile under anti-phase diffraction conditions, as well as from a comparison of the in- and anti-phase scattering intensities, is

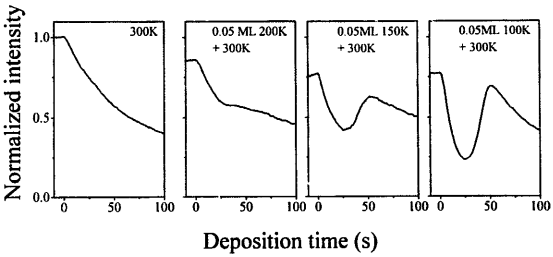

Fig. 4. Evolution of the normalized anti-phase He intensities during deposition of Cu at $T=300$ K onto Cu(111) surfaces, which were treated by pre-deposition of 0.05 ML Cu at lower temperatures as indicated. Deposition was carried out at a rate of $R=0.02$ ML/s.

~430 Å. This length being of the same order as the transfer width of our instrument, is the origin of the fact that the anti-phase intensity after deposition of 0.5 ML is higher than zero. This latter consideration would modify our estimate for the degree of completion of the first layer after deposition of 1 ML only slightly, since at this coverage small changes in the intensity are only mildly expressed in the layer distribution. The length scale obtained for growth subsequent to pre-deposition at 100 K corresponds to an increase of the island density by a factor of at least 8 with respect to the unmanipulated growth at 300 K. It must be kept in mind, though, that unmanipulated growth at 300 K on our surface leads to structures of the order of the terrace width. Island sizes may thus be limited by the mean terrace width on the surface. The island density enhancement factors may therefore be larger with respect to unmanipulated growth on a "perfect" surface.

3.2.2. Growth manipulation via ion beam pulses

A second and more convenient way of creating an artificially high density of nuclei is to bombard the surface with ions prior to or during the first stages of deposition. During bombardment, the surface is not only sputtered, but also adatoms are created due to displacement of atoms by collisions and upward diffusion of bulk interstitials. These so called "target" adatoms have been directly observed with STM for Pt(111) [44–46], for Ag(111) [25] and for Cu(100) [47,48]. At temperatures high enough to allow adatom diffusion, the adatoms created in direct vicinity to the ion impact site form one or several adatom islands close to the impact site [45]. These then serve as nucleation centres during film growth.

The normalized in- and anti-phase He-intensities recorded during a series of growth experiments at 300 K are shown in Fig. 5. In these experiments, the freshly prepared surfaces were bombarded with 1.2 keV Ne^+-ions using fluences Q between 5×10^{15} and 1.5×10^{17} ions/m^2, as indicated. These fluences correspond to sputtering of 0.001 to 0.03 ML respectively [49]. Immediately after ion bombardment, Cu deposition was started at a rate of $R=0.02$ ML/s. From Fig 5 it is clear that ion bombardment indeed results in the two-dimensional growth of one monolayer for all ion fluences used.

The exact shape of the in- and anti-phase curves varies, however, with the ion fluence. In order to clarify the origin of this variation we took anti-phase peak profiles from surfaces onto which 0.5 ML were deposited after ion bombardment.

A typical example is shown in the inset of Fig. 6, where the reflected He intensity is plotted versus the momentum transfer parallel to the surface. From the ring-like broadening in the peak profiles, the typical length scale of the structures, i.e., the mean adatom island separation, was derived as a function of the ion fluence. As can be seen from Fig. 6, the length scale falls with rising ion fluence until at a fluence of $Q\approx8\times10^{16}$ ions/m^2 a saturation in the length scale of ~300 Å is reached. A further increase of the ion fluences by roughly a

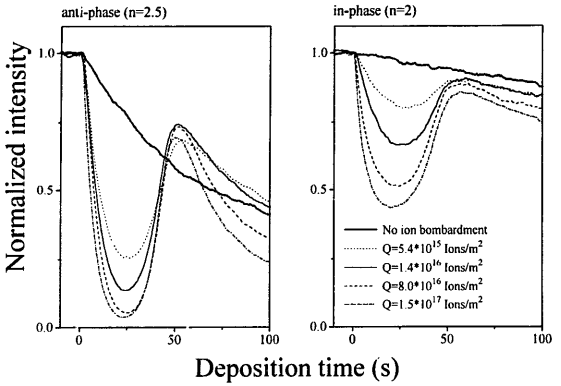

Fig. 5. Normalized in- and anti-phase He intensities during deposition of Cu at $T=300$ K onto surfaces which were treated by ion bombardment with fluences as indicated. Deposition was carried out at a rate of $R=0.02$ ML/s.

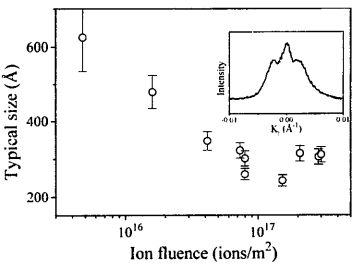

Fig. 6. Typical structure sizes after deposition of 0.5 ML Cu onto surfaces, which were treated by ion bombardment, as a function of fluence. The sizes were evaluated from the broadening of anti-phase peak profiles, an example of which is shown in the inset. The given error bars represent the error resulting from fitting the peak profiles. Deposition was carried out at a rate of $R=0.02$ ML/s.

factor of five does not lead to growth of significantly smaller structures on the surface. An efficient enhancement of the island density under the chosen growth condition requires, therefore, bombarding with an ion fluence of at least $Q=8\times10^{16}$ ions/m^2. Lower fluences obviously lead to less effective manipulation of nucleation.

We now return to the detailed examination of the curves shown in Fig. 5, starting with the anti-phase curves. For the two lowest fluences ($Q=5\times10^{15}$ and $Q=1.4\times10^{16}$ ions/m^2) the sizes of the structures are considerably larger than the transfer width. This would explain the rather high anti-phase intensity at the minimum (0.5 ML coverage), even if growth were perfect 2D. At 1 ML coverage, however, the anti-phase intensity for the lowest ion fluence is lower than that for higher ion fluences, indicating that the film is rougher than the others. We conclude that the island density created by bombarding with this low ion fluence is too low in order to efficiently suppress nucleation on top of islands and insure sufficient interlayer mass transport. Increasing the ion fluence leads to smaller structures and the anti-phase intensity at 1 ML coverage increases, indicating a better interlayer mass transport and a more perfect 2D growth. The intensity at the minimum (0.5 ML) decreases with ion fluence both due to the better 2D growth and to the decrease in length scale with respect to the transfer width. For the highest ion fluence shown in Fig. 5 ($Q=1.5\times10^{17}$ ions/m^2), however, the anti-phase intensity at both 0.5 and 1 ML coverage is slightly lower than the intensity for $Q=8\times10^{16}$ ions/m^2. Since this cannot be attributed to a change in length scale, we assume

that some ion bombardment induced defects remain in the layer. These defects should be visible also in the in-phase intensity.

When examining the in-phase intensities one notices that, indeed, the intensities at one monolayer coverage and beyond decrease with increasing ion fluence, indicating that the layer contains more defects. As this trend also holds for the higher ion fluences, which give rise to similar island densities, we assume that these defects are not only related to the different morphology of the layers, but contain some contribution from ion bombardment induced defects, which do not anneal even at higher coverage. These defects could either be small vacancy islands created by the sputtering or crystal defects underneath the surface such as implanted neon atoms.

We conclude that bombardment is best done with the minimal ion fluence with which the saturation length scale can be obtained. This ensures that the optimal island density is obtained, while minimizing the amount of residual defects.

Returning to the examination of anti-phase intensity curves beyond one monolayer coverage, one notices that not only the absolute value, but also the *slope* of the decay of the signal varies with ion fluence (or rather with structure size, as it is similar for the two highest fluences). This indicates that there is a difference in morphology of the layers in addition to the different amount of left-over sputter defects. Presumably, this has to do with a partial "transfer" of the length scale established in the first layer, to the second one. As the first monolayer is not completely filled upon coalescence, some holes still remain between the islands. The distribution of these holes reflects the characteristic length scale of the first monolayer, which slightly influences the growth of the second layer. This so called "memory" effect was also observed for manipulated growth of Ag on Ag(111) [50].

Assuming an ideal instrument and a three-layer-system, the anti-phase intensity for the ion fluence $Q=8\times10^{16}$ ions/m^2 (removal of only 0.016 ML), at 1 ML coverage corresponds to a filling of the first layer of 96%. This result is even better than that obtained by pre-deposition at the lowest temperature. The typical length scale of the structures obtained with this ion fluence gives an enhancement factor of 16 in the island density, which is larger than that obtained by pre-deposition at low temperatures, in accord with the better growth.

A comparison of the two growth manipulation procedures – pulsed ion bombardment and temperature alternation – is clearly in favour of the pulsed bombardment procedure, which easily allows higher enhancement factors. Another advantage of this procedure is the easy applicability to the growth of many monolayers. Fig. 7 displays the anti-phase He-intensity during deposition of 50 ML copper ($R=0.02$ ML/s, $T=300$ K). Here, an ion pulse was given during deposition just when growth in a given layer started. In this way the island density is enhanced in each layer and the film grows two-dimensionally. The inset in Fig. 7 shows in detail the first few oscillations and as a comparison the curve which corresponds to unmanipulated growth with the same growth parameters. It can clearly be seen that the anti-phase intensity upon monolayer completion is higher for the manipulated growth than for the unmanipulated one even after deposition of a "thick" film. This method therefore enables growth of smooth

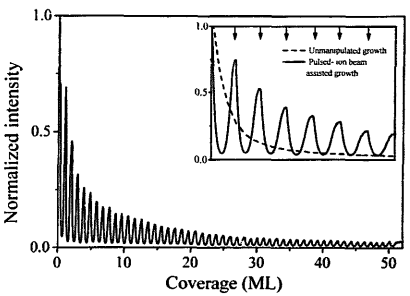

Fig. 7. Normalized He anti-phase intensity as a function of Cu coverage at $T=300$ K and a rate of $R=0.02$ ML/s. Deposition was intermitted by ion bombardment at the initial stages of growth of each layer. The evolution of the anti-phase He intensity during deposition of the first couple of monolayers is displayed in the inset, and compared with the intensity obtained during unmanipulated growth. Ion bombardment is indicated by arrows in the inset.

films many monolayers thick. Similar results were obtained when bombardment was carried out using 600 eV argon ions instead of neon.

3.3. Oxygen mediated growth

It has long been reported in the literature that the introduction of foreign substances to an epitaxial system can affect the growth mode in hetero- as well as homo-epitaxy [19,51–57]. For example, Sb changes the growth mode in the Ag/Ag(111) system from three- to two-dimensional [19].

One of the substances which is known to influence growth in noble-metal and other systems is oxygen [55–57]. Experiments on the growth of Pt on Pt(111) [55,56] show that growth in that system is improved when oxygen is used as a surfactant. It was also demonstrated that in the Pt/Pt(111) case oxygen floats up to the highest uncovered layer as deposition is continued. For growth of Pt on Pt(111) it was shown that oxygen influences the growth by reducing the step-edge barrier and thus facilitating interlayer mass transport [56].

Reports on the influence of O_2 on growth of Cu on Cu(111) indicate that exposure to oxygen prior to deposition (pre-exposure) might improve growth in this system also. Dastoor and co-workers [21] observed He intensity oscillations during Cu deposition on Cu(111) at a narrow temperature range around 200 K.

We first concentrate on experiments carried out at 300 K, with different oxygen pre-exposures between 2 and 110 Langmuir (L). Under our experimental conditions, O_2 is reported to chemisorb on Cu(111) dissociatively, forming a disordered layer [58,59]. Desorption does not take place at temperatures below 620 K [58]. The oxygen atoms are situated on or within the topmost copper layer [60,61].

Following low (2 L) as well as high (110 L) oxygen exposures no oscillation in He intensity during deposition of copper could be observed. For a limited range of O_2 exposures ($\sim 36-\sim 72$ L), oscillations as a function of Cu deposition were found.

Our main conclusion is that although O_2 pre-exposure does lead to small oscillations in the He intensity as a function of deposition, oxygen is nevertheless quite ineffective in promoting growth of smooth two-dimensional films. Fig. 8 depicts the evolution of the $n=2.5$ normalized anti-phase He reflection during Cu deposition at 300 K following O_2 exposures as indicated. The main features of the behaviour are a strong decrease in the intensity upon Cu deposition, followed by a couple of minute oscillations, sometimes superimposed on a slight gradual intensity increase. The period of the oscillations, from the second maximum onward is more or less constant and corresponds roughly to monolayer coverage. The best growth is achieved after 72 L exposure. We estimate the oxygen coverage on the surface following that exposure to be about 5–7% ML from the evaluation of Auger electron spectroscopy (AES) data following the procedure in Ref. [60].

O_2 exposure was adjusted to obtain He intensity oscillations during Cu deposition at 300 K. When both O_2 exposure and Cu deposition were carried out at either 200 or 400 K, no oscillations were observed. However, we did observe oscillations during Cu deposition at these temperatures when the pre-exposure of oxygen was done at 300 K. We conclude that the decisive factor is the amount of adsorbed oxygen on the surface, which is strongly temperature dependent.

Two possible principal mechanisms could be responsible for the partially two-dimensional character of the growth. One is a reduction of the step-edge barrier, similar to the case of Pt/Pt(111), the second is a buildup of an increased island density on the substrate due to an oxygen-induced restricted mobility [17,24]. In both cases monolayer completion should be followed by an up-"swim" of the oxygen from the lower to the upper layer.

In order to distinguish between the two mechanisms, we exposed to O_2 surfaces onto which 0.05 ML Cu were pre-deposited at a low temperature (100 K), and examined the subsequent growth at 300 K. Fig. 9 shows the results of two such experiments, where the surface was treated by a low (1 L) as well as by a higher (36 L) O_2 exposure. These experiments are identical, apart from the O_2 exposure, to that carried out to obtain the result in the right hand panel in Fig. 4, which is

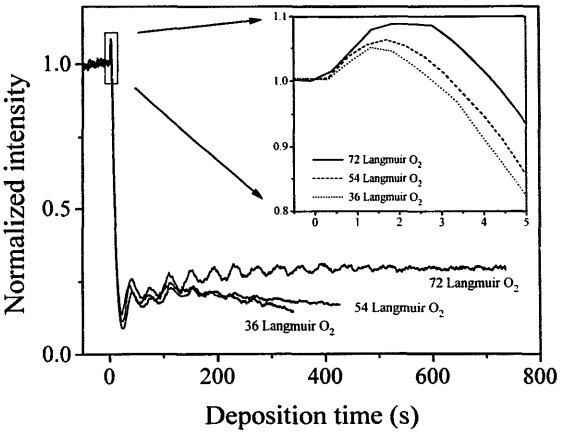

Fig. 8. Normalized He anti-phase intensity as a function of Cu deposition time at $T=300$ K onto surfaces which were treated by O_2 pre-exposure as indicated. The initial stages of Cu deposition are shown in detail in the inset.

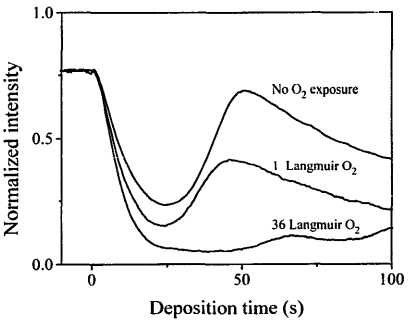

Fig. 9. Normalized He anti-phase intensity as a function of Cu deposition time at $T=300$ K. Prior to oxygen exposure and deposition at room temperature 0.05 ML Cu were deposited onto all surfaces at 100 K. The two lower curves were taken from a surface which were additionally treated by 1 and 36 L O_2 exposure, as indicated.

presented again in Fig. 9 for ease of comparison. Had oxygen reduced the step edge barrier, the interlayer mass transport after O_2 exposure would have been much improved due to the combined effect of reduction in the length scale formed by pre-deposition, and the reduced barrier. The resulting layer would have been flatter than the one obtained without O_2 exposure, and the He intensity after deposition of a full monolayer would have been higher. Obviously, this is not the case. The layers grown after O_2 exposure are rougher than the layer grown directly on the surface with pre-deposited islands. We conclude that the oxygen induced oscillations are not a result of a reduction of the step edge barrier.

The alternative mechanism involves reduction in the length scale of the islands formed on the substrate due to a reduced mobility in the presence of oxygen. Evaluation of anti-phase peak profiles at 0.5 ML coverage shows that the length scale of islands formed as a result of deposition in the presence on oxygen is indeed smaller than that formed during unmanipulated growth. The estimated mean island separation at room temperature is about 400 Å.

In order to influence the growth of more than one or two monolayers, the oxygen has to float up during deposition. The oxygen AES signal from the surface after deposition of 15 ML Cu was

found indeed to be identical within the sensitivity of our AES to that obtained from the surface directly after O_2 exposure. AES studies of O_2 mediated growth of Cu on Ru(0001) reveal a similar floating [57].

The two-dimensional aspect of the growth can thus be explained by a restriction of the mobility of Cu adatoms in the presence of oxygen on the surface. This leads to an increase in island density, in a similar manner to the modus operandi of the growth-manipulation techniques discussed in the former sections of this paper.

A closer look into the details of the deposition curves reveals, however, that the interaction of oxygen with copper and the dynamics of growth during Cu deposition are actually far from being simple. To mention some of the unconventional features: (1) Immediately upon Cu deposition, an increase in the He intensity is observed. The time elapsed until reaching the maximum of this increase is a function of O_2 exposure as demonstrated in the inset of Fig. 8. This was also observed by Dastoor and co-workers [21]. (2) The period of the first oscillation is smaller than that of the subsequent ones. (3) The amplitude of the second oscillation is lower than that of the others. (4) The first maximum is totally missing when depositing on surfaces which were treated by Cu pre-deposition, and O_2 exposure (see Figs. 9 and 10a). Most interestingly, interruption of deposition during the first oscillation, and continued deposition after a few minutes does *not* result in the completion of the original interrupted oscillation, but rather in the appearance of a new, complete, oscillation, having the "normal" period (see Fig. 10b). This effect does not occur when oxygen is not present on the surface, and 2D growth is induced by e.g. pulsed ion bombardment.

The general picture emerging is that nucleation of oxygen containing islands takes place upon Cu deposition. This stage is accompanied by the small increase in the He intensity, as the oxygen is no longer freely distributed on the terrace. Continued deposition produces a very rough oxygen-containing layer, within which rearrangement of the oxygen position is possible during the time scale of the experiment. This stage is accompanied by a strong decrease in He intensity. Rearrangement

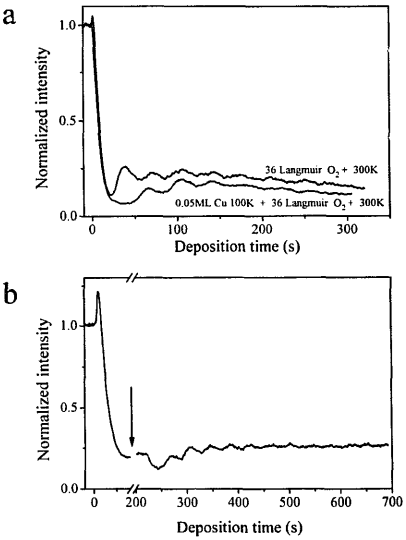

Fig. 10. (a) Normalized He anti-phase intensity as a function of Cu deposition time at $T=300$ K onto surfaces which were treated by 36 langmuir O_2 exposure. The lower curve was taken from a surface onto which 0.05 ML Cu were deposited at 100 K prior to O_2 exposure. (b) Normalized He anti-phase intensity as a function of Cu deposition at $T=300$ K after 36 langmuir O_2 exposure. Deposition was interrupted as indicated by the arrow, and continued after a couple of minutes.

presumably continues during the time needed to complete one or two oscillations, and results in the unconventional features occurring during the first two oscillations. On the resultant rough surface, mobility of copper adatoms is restricted, and oscillations in the He intensity can be observed. Oscillations persist as the oxygen is able to float up to the growth front. With increasing deposition, the initial roughness of the surface may be partially smoothened out, and the reflected intensity increases slightly in some cases.

The details of oxygen interaction, and especially the dynamics during the initial stages of Cu deposition are, in our belief, quite complex, and deserve a more thorough examination which is beyond the

scope of the present paper. These questions may well be better addressed using real-space techniques.

Acknowledgements

N.N. Lipkin is thankful for support by the Alexander von Humboldt Foundation and for the Marie Curie Fellowship by the Commission of the European Communities.

References

[1] D.K. Flynn-Sanders, J.W. Evans and P.A. Thiel, Surf. Sci. 289 (1993) 75; H.C. Kang, D.K. Flynn-Sanders, P.A. Thiel and J.W. Evans, Surf. Sci. 256 (1991) 205.
[2] S.T. Purcell, B. Heinrich and A.S. Arrott, Phys. Rev. B 35 (1987) 6458; E. Kopatzki, S. Gunther, W. Nichtl-Pecher and R.J. Behm, Surf. Sci. 284 (1993) 154.
[3] J.J. de Miguel, A. Sánchez, A. Cebollada, J.M. Gallego, J. Ferrón and S. Ferrer, Surf. Sci. 189/190 (1987) 1062; H.J. Ernst, F. Fabre and J. Lapujoulade, Surf. Sci. 275 (1992) L682.
[4] W.F. Egelhoff, Jr. and I. Jacob, Phys. Rev. Lett. 62 (1989) 921.
[5] H.A. van der Vegt, W.J. Huisman, P.B. Howes and E. Vlieg, Surf. Sci. 330 (1995) 101.
[6] P. Bedrossian, B. Poelsema, G. Rosenfeld, L.C. Jorritsma, N.N. Lipkin and G. Comsa, Surf. Sci. 334 (1995) 1.
[7] Y. Suzuki, H. Kikuchi and N. Kosizuka, Jpn. J. Appl. Phys. 27 (1988) L1175.
[8] R. Kunkel, B. Poelsema, L.K. Verheij and G. Comsa, Phys. Rev. Lett. 65 (1990) 733.
[9] B. Poelsema, R. Kunkel, N. Nagel, A.F. Becker, G. Rosenfeld, L.K. Verheij and G. Comsa, Appl. Phys A 53 (1991) 369.
[10] M. Bott, T. Michely and G. Comsa, Surf. Sci. 272 (1992) 161.
[11] B. Poelsema, A.F. Becker, R. Kunkel, G. Rosenfeld, L.K. Verheij and G. Comsa, Springer Proceedings in Physics, Vol. 73, Eds. R.F. Howe, R.N. Lamb and K. Wandelt (Springer, Berlin, 1993) p. 95.
[12] M. Henzler, T. Schmidt and E.Z. Luo, The Structure of Surf.s IV, Eds. X.D. Xie, S.Y. Tong and M.A. Van Hove (World Scientific, Singapore, 1994) p. 619.
[13] G. Ehrlich and F.G. Hudda, J. Chem. Phys. 44 (1966) 1039.
[14] R.L. Schwoebel and E.J. Shipsey, J. Appl. Phys. 37 (1966) 3682.
[15] M. Bott, M. Hohage, T. Michely and G. Comsa, Phys. Rev. Lett. 70 (1993) 1489.
[16] T. Michely, M. Hohage, S. Esch and G. Comsa, Surf. Sci., to be published.
[17] G. Rosenfeld, R. Servaty, C. Teichert, B. Poelsema and G. Comsa, Phys. Rev. Lett. 71 (1993) 895.
[18] K. Meinel, M. Klaua and H. Bethge, J. Cryst. Growth 89 (1988) 477; K. Meinel, M. Klaua and H. Bethge, Phys. Status Solidi 110 (1988) 189.
[19] H.A. van der Vegt, H.M. van Pinxteren, M. Lohmeier, E. Vlieg and J.M.C. Thornton, Phys. Rev. Lett. 68 (1992) 3335.
[20] P.C. Dastoor, J. Ellis, A. Reichmuth, H. Bullman, B. Holst and W. Allison, Surf. Rev. Lett. 1 (1994) 509.
[21] P.C. Dastoor, PhD Thesis, Cambridge, 1994.
[22] M. Henzler, Prog. Surf. Sci. 42 (1993) 297.
[23] M. Henzler, Surf. Sci. 298 (1993) 369.
[24] G. Rosenfeld, B. Poelsema and G. Comsa, J. Cryst. Growth 151 (1995) 230.
[25] G. Rosenfeld, N.N. Lipkin, W. Wulfhekel, J. Kliewer, K. Morgenstern, B. Poelsema and G. Comsa, Appl. Phys. A61 (1995) 455.
[26] B. Poelsema and G. Comsa, Scattering of Thermal Energy Atoms, Springer Tracts in Modern Physics, Vol. 115 (Springer, Berlin, 1989).
[27] B. Poelsema, G. Mechtersheimer and G. Comsa, Surf. Sci. 111 (1981) 519.
[28] R. Kunkel, PhD Thesis, Jülich, 1991.
[29] An estimate of the average terrace width $\bar{A}$ is given by

$$\bar{A} \approx \frac{\lambda_{He}}{\Delta\vartheta_f}\left[\sqrt{\left(\frac{1+\cos^2\vartheta_i}{2}\right)^2+\cos^2\vartheta_i\left(\left(\frac{I^{in}}{I^{anti}}\right)^2-1\right)}-\frac{1+\cos^2\vartheta_i}{2}\right]^{-\frac{1}{2}}$$

where λ_{He} is the wavelength of the He-beam, $\Delta\vartheta_f$ is the full width at half maximum (FWHM) of the direct He-beam, ϑ_i is the diffraction angle under in-phase conditions, I^{in} and I^{anti} are the reflected He-intensities under in- and anti-phase diffraction conditions [28].
[30] M. Henzler, Appl. Surf. Sci. 11/12 (1982) 450.
[31] J. Wollschläger, J. Falta and M. Henzler, Appl. Phys. A 50 (1990) 57.
[32] The slight decay of the anti-phase He intensity durig deposition at 450 K may be attributed to kinetic roughening of the pre-existing steps in the step flow growth mode.
[33] M. Henzler, private communication.
[34] J.A. Venables, Phil. Mag. 27 (1973) 697.
[35] J.A. Venables, G.D.T. Spiller and M. Hanbücken, Rept. Prog. Phys. 47 (1984) 399.
[36] H.J. Ernst, F. Fabre and J. Lapujoulade, Surf. Sci. 275 (1992) L682.
[37] J. Jacobsen, K.W. Jacobsen, P. Stoltze and J.K. Nørskov, Phys. Rev. Lett. 74 (1995) 2295.
[38] M. Villarba and H. Jonsson, Phys. Rev. B 49 (1994) 2208; M. Villarba and H. Jonsson, Surf. Sci. 317 (1994) 15.
[39] Yinggang Li and A.E. DePristo, Surf. Sci. 319 (1994) 141.
[40] Yinggang Li and A.E. DePristo, to be published.
[41] G. Meyer, J. Wollschläger and M. Henzler, Surf. Sci. 231 (1990) 64.
[42] P. Stoltze, J. Phys. Condens. Matter 6 (1994) 9495.

[43] For a three-layer system, the coverage of the first layer close to 1 monolayer completion is given by: $\theta_1=\frac{1}{3}(1+2\theta+\sqrt{I^{anti}/I^{anti}_0})$, where I^{anti}/I^{anti}_0 is the normalized scattered intensity under anti-phase diffraction conditions.
[44] T. Michely and G. Comsa, Phys. Rev. B. 44 (1991) 8411.
[45] T. Michely and C. Teichert, Phys. Rev. B 50 (1994) 11156.
[46] C. Teichert, M. Hohage, T. Michely and G. Comsa, Phys. Rev. Lett. 72 (1994) 1682.
[47] M. Breeman and D.O. Boerma, Surf. Sci. 278 (1992) L110.
[48] J.C. Girard, Y. Samson, S. Gauthier, S. Rousset and J. Klein, Surf. Sci. 302 (1994) 73.
[49] At 440 K ion bombardment results in layer-by-layer etching causing oscillations of the anti-phase intensity. These oscillations allow to relate the ion fluence to the overall amount of material, that is removed from the substrate. A similar behaviour for Pt(111) during sputtering has been previously reported by B. Poelsema, L.K. Verheij and G. Comsa, Phys. Rev. Lett. 53 (1984) 2500.
[50] G. Rosenfeld, PhD Thesis, Jül-2914, (Jülich 1994).
[51] W.F. Egelhoff, Jr. and D.A. Steigerwald, J. Vac. Sci. Technol. A 7 (1989) 2167.
[52] M. Copel, M.C. Reuter, E. Kaxiras and R.M. Tromp, Phys. Rev. Lett. 63 (1989) 632.
[53] M. Horn-von Hoegen, F.K. LeGoues, M. Copel, M.C. Reuter and R.M. Tromp, Phys. Rev. Lett. 67 (1991) 1130.
[54] N. Gradjean, J. Massies and V.H. Etgens, Phys. Rev. Lett. 69 (1992) 796.
[55] B. Poelsema, R. Kunkel, N. Nagel, A.F. Becker, G. Rosenfeld, L.K. Verheij and G. Comsa, Appl. Phys. A 53 (1991) 369.
[56] S. Esch, M. Hohage, T. Michely and G. Comsa, Phys. Rev. Lett. 72 (1994) 518.
[57] H. Wolter, M. Schmidt and K. Wandelt, Surf. Sci. 298 (1993) 173; M. Schmidt, H. Wolter and K. Wandelt, Surf. Sci. 307–309 (1994) 507; K. Kalki, M. Schick, G. Ceballos and K. Wandelt, Thin Solid Films 228 (1993) 36.
[58] G. Ertl, Surf. Sci. 6 (1967) 208.
[59] L.H. Dubois, Surf. Sci. 119 (1982) 399.
[60] H. Niehus, Surf. Sci. 130 (1983) 41.
[61] R.W. Judd, P. Hollins and J. Pritchard, Surf. Sci. 171 (1986) 643.